Meta-Boolean models of asymmetric division patterns in the *C. elegans* intestinal lineage

Implications for the posterior boundary of intestinal twist

Sofia Pettersson,* Robert Forchheimer and Jan-Åke Larsson

Division of Information Coding; Department of Electrical Engineering; Linköping University; Linköping, Sweden

The intestine of *Caenorhabditis elegans* is derived from 20 cells that are organized into nine intestinal rings. During embryogenesis, three of the rings rotate approximately 90 degrees in a process known as intestinal twist. The underlying mechanisms for this morphological event are not fully known, but it has been demonstrated that both left-right and anterior-posterior asymmetry is required for intestinal twist to occur. We have recently presented a rule-based meta-Boolean tree model intended to describe complex lineages. In this report we apply this model to the E lineage of *C. elegans*, specifically targeting the asymmetric anterior-posterior division patterns within the lineage. The resulting model indicates that cells with the same factor concentration are located next to each other in the intestine regardless of lineage origin. In addition, the shift in factor concentrations coincides with the boundary for intestinal twist. When modeling *lit-1* mutant data according to the same principle, the factor distributions in each cell are altered, yet the concurrence between the shift in concentration and intestinal twist remains. This pattern suggests that intestinal twist is controlled by a threshold mechanism. In the current paper we present the factor concentrations for all possible combinations of symmetric and asymmetric divisions in the E lineage and relate these to the potential threshold by studying existing data for wild-type and mutant embryos. Finally, we discuss how the resulting models can serve as a basis for experimental design in order to reveal the underlying mechanisms of intestinal twist.

Introduction

The intestine of *Caenorhabditis elegans* is exclusively derived from 20 cells originating from the E founder cell, a blastomere that is born at the eight-cell stage of the embryo.[1-4] The fate of the intestinal lineage is determined through a series of asymmetric divisions resulting in activity of the maternal transcription factor SKN-1 in EMS; the mother of the E blastomere.[5] The signaling cascade beginning with SKN-1 acts together with an extracellular signaling event that polarizes EMS to restrict the endoderm fate to the E blastomere, culminating in the activation of the GATA factor ELT-2, a key regulator of the intestinal fate.[5-10] The various stages of intestinal development are described by referring to the number of intestinal cells present at the time (E1-E20). For example, the E8 stage represents the developmental stage where eight E cells are present. With the exception of a symmetric left-right cell division at the E2 stage, cell divisions in the lineage occur along the anterior-posterior axis and are asymmetric, resulting in anterior-posterior asymmetric distribution patterns of various proteins and transcription factors.[1,11-13]

The spatial arrangement of the endoderm precursors during embryonic development has been described in detail elsewhere and will only be discussed briefly here.[1,2] In short, the 20 cells of the intestine are eventually organized into nine rings (Int I-IX). With one exception, descendants of the anterior daughter of the E blastomere make up the forward part of the intestine (Int I-III and V) while the posterior part of the intestinal tube originates from the posterior daughter, Ep (Int IV, VI-IX). During development, three of the forward intestinal rings (Int II-IV) turn approximately 90° counterclockwise in a process known as intestinal twist.[2] The underlying mechanisms governing this morphological phenomenon are not fully known, yet two asymmetries within the E lineage have been shown to influence the event. First, a left-right asymmetry that is established through an external Notch cell-signaling event at the E4 stage is crucial for twist to occur.[14] The downstream target of this Notch signal, which is further relayed within the intestine at the E16 stage, has been identified as the REF-1 transcription factor.[15,16] Second, *lit-1* activity seems to affect the posterior boundary of intestinal twist.[14] The LIT-1 protein is part of a Wnt/β-catenin complex that establishes anterior-posterior asymmetries in the *C. elegans*
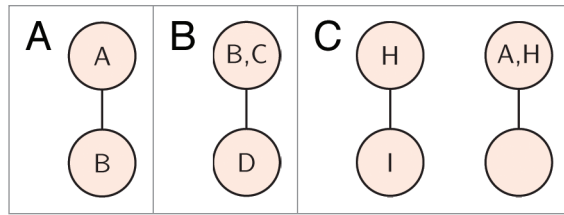
Figure 1. Example of the notation used for regulator functions. (**A**) The regulator g(B|A) denotes that factor *B* will be produced if factor *A* is present in the previous time step. (**B**) Synergy can be modeled by using regulators on the form g(D|B,C) where factor *D* will be produced only if both factor *B* and *C* are present. (**C**) Repression can be modeled in a similar manner. The regulator g(I|H,–A) describes the production of factor *I* when factor *H* is present given that factor *A* is not. From Larsson et al.[20]
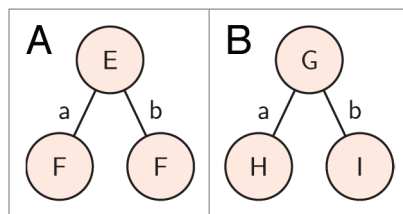

Figure 2. Cell division is controlled by the cell division factors *a* and *b*. (**A**) The regulators g(a,b|E), g(F|E) initiate cell division when *E* is present in the mother cell and the symmetric production of factor *F* in both daughter cells. (**B**) Asymmetric cell division is described using *a* and *b*. The regulators g(a,b|G), g(H|G,a) and g(I|G,b) describe the asymmetric production of factors *H* and *I* in the two daughter cells. From Larsson et al.[20]

embryo by controlling the transcriptional activity of POP-1, yet how the anterior-posterior asymmetry patterns influence intestinal twist remains unclear.[17-19]

We have recently presented a rule-based low-complexity meta-Boolean model designed for large cell lineage trees.[20] In short, the model utilizes a factor framework to describe the properties of a given cell in the tree. These factors can represent a range of different physical factors, or even groups thereof, such as intracellular proteins (i.e., transcription factors), extracellular signals (such as cell-to-cell signaling events) or other physical cues (such as external pressure). The modeling technique can incorporate synergies between model factors and is able to describe the dynamic behavior of genetic regulatory networks. The low complexity allows for larger systems such as complete embryonic lineage trees to be modeled, and the model is intended to enable investigation of the general patterns that arise in such large systems. For example, it has been used to indicate where in lineage trees asymmetry breaking may be controlled by external influences.[20] In our previous work, we have shown that the meta-Boolean model is able to faithfully describe the embryonic cell lineage of the nematode *C. elegans*.[20] We now focus on a more limited part of this model organism, the intestine or endoderm (reviewed in ref. 21).[21]

The aim of this study is to establish general asymmetric cell division models of the E lineage in order to understand the role of anterior-posterior asymmetry in intestinal twist.

The Meta-Boolean Cell Lineage Model

Factor content, synergy and repression. The meta-Boolean model utilizes a factor framework to describe the properties and state of a given cell, represented as a node in the lineage tree. In addition, the factor content of a cell at a specific time determines the factor content of the cells in the following time step. For the purposes of this article, time is discretized at cell division, a natural choice for cell lineage modeling, yet nothing prevents the use of a more fine-grained time scale to capture events occurring in between divisions. To describe this sequential factor production, we use rule-based regulator expressions on the form

$$g(B|A),$$

which reads "Factor *B* will be produced given that factor *A* is present in the previous time step" (**Fig. 1A**). Through this notation, synergy can easily be incorporated through a 'logical AND'. With the below regulator expression, factor *D* will be produced only if both factor *B* and factor *C* are present (**Fig. 1B**)

$$g(D|B,C).$$

Similarly, the 'logical NOT' can be used to describe production of a factor given that another factor, for instance a repressor, is not present. Here, the regulator expression states that factor *I* will be produced if factor *H* is present only when factor *A* is not present (**Fig. 1C**)

$$g(I|H,-A).$$

Discrete factor concentrations. Cell fate decisions are dependent on the sequential activation of specific transcription factors. These activations can be dependent on the mere presence of an activator, but in some cases the concentration of the activator is critical. This can be incorporated in the meta-Boolean model via discrete factor concentrations where, rather than introducing new factors in each node, various levels of the same factor is used to describe the properties of the nodes. From a biological point of view, discrete factor concentrations can also be used to model the dynamics of transient factors, such as the onset, peak expressions and downregulation of transcription factors.[22] This means that production of subsequent factors can be modeled based on the concentration of a given factor, such as a critical threshold, rather than simply the presence of it. Furthermore, by combining discrete factor concentrations and synergy, the ratio between two factors can be incorporated as a condition for factor production. In this manner, the appropriate balance between an activator and a repressor can be modeled.

Symmetric and asymmetric cell division. It is crucial for any cell lineage model to incorporate mechanisms that handle both symmetric and asymmetric cell divisions. In the meta-Boolean model, this is accomplished by assigning two specific cell division factors, *a* and *b* (**Fig. 2A**). These factors are produced simultaneously, initiate cell division and then immediately disappear

$$g(a, b|E),$$
$$g(F|E).$$

The above regulator expressions describe a symmetric division. Here, cell division is initiated in a cell, containing factor *E*, which divides symmetrically into two daughter cells in which factor *F* is produced as a consequence of the presence of factor *E* in the mother cell. Importantly, the two cell division factors *a*

and *b* are not intended to mirror actual factor content (transcription factors, etc.). Rather, they are formal markers for the physical distinction between the two daughter cells. As such, they can be used to model asymmetric cell division by adding them to the conditions for factor production. The below regulator expressions describe a scenario where a cell containing the factor *G* divides into two distinct daughters. Factor *H* is produced only in the left-hand daughter and factor *I* is produced only in the right-hand daughter (**Fig. 2B**)

$$g(a,b|G),$$
$$g(H|G,a),$$
$$g(I|G,b).$$

Asymmetric distribution. The cell division in **Figure 2B** describes the asymmetric production of two separate factors, one in each daughter cell. A different mechanism by which two different daughter cells can be established is the polarization of the cellular content prior to cell division. This is the case for the mother of the E blastomere, EMS. It receives an external signal from the P$_2$ cell in the 4-cell embryo, resulting in the polarization and later asymmetric cell division of the EMS cell.[6,8] Such asymmetric divisions can be modeled using the following regulator expressions (**Fig. 3A**)

$$g(a,b|A,B),$$
$$g(A|A,B,a),$$
$$g(B|A,B,b).$$

In this case, the regulator functions describe the asymmetric distribution of factors rather than production of the same. An incomplete polarization of proteins, i.e., transcription factors and/or their repressors, where different amounts of the protein is obtained in the two daughter cells, can be modeled using the following notation (**Fig. 3B**)

$$g(a,b|A),$$
$$g(0.9A|A,a),$$
$$g(0.1A|A,b).$$

Here, the factor amounts in the daughter cells are assigned to specific levels. A more general notation to describe the distribution of the content in the mother cell, the factor *A*, is found below (**Fig. 3C**)

$$g(mA|A,a),$$
$$g(nA|A,b).$$

In this case, *m* and *n* describe the portion of the initial amount of factor *A* (= 1) that is distributed to each daughter (where *m* + *n* = 1, 0 ≤ *m*, *n* ≤ 1). A perhaps more relevant option is to model the factor concentrations (factor amount per volume) for the daughter cells (**Fig. 3D**.

$$g(xA|A,a),$$
$$g(yA|A,b).$$

Here *x* equals the amount of factor *A* that is distributed to the anterior daughter (= *m*) divided by the volume of this daughter cell. For volume-symmetric cell divisions, where the original cell volume is halved, *x = 2m* and *y = 2n*, from which follows that *x + y = 2* and *0 ≤ x, y ≤ 2*. For the remainder of this paper, all divisions will be considered volume-symmetric unless otherwise stated. Volume-asymmetric cell divisions can be modeled in a similar manner, if the relationship between *x* and *y* discussed above is adjusted accordingly.
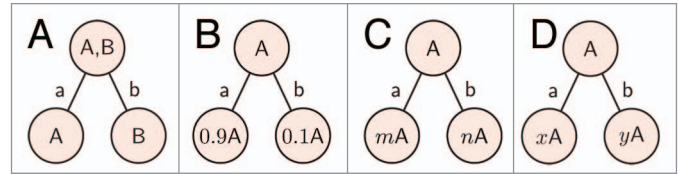

Figure 3. Various ways to model asymmetric cell division. (**A**) Cell division following polarization, where two factors, *A* and *B*, are separated to the two daughter cells, can be modeled using the regulators g(a,b|A,B), g(A|A,B,a) and g(B|A,B,b). (**B**) An incomplete polarization of factor *A* can be modeled using the regulators g(a,b|A), g(0.9A|A,a) and g(0.1A|A,b). (**C**) The regulators g(a,b|A), g(mA|A,a) and g(nA|A,b) describe asymmetric distribution of factor *A* to its daughter cells, giving the anterior daughter *m* times and the posterior daughter *n* times the initial amount of the factor, where *m + n = 1* and *0 ≤ m,n ≤ 1*. (**D**) For volume-symmetric cell divisions, the factor concentrations (amount per volume) are described by g(a,b|A), g(xA|A,a) and g(yA|A,b), where *x + y = 2* and *0 ≤ x,y ≤ 2*.
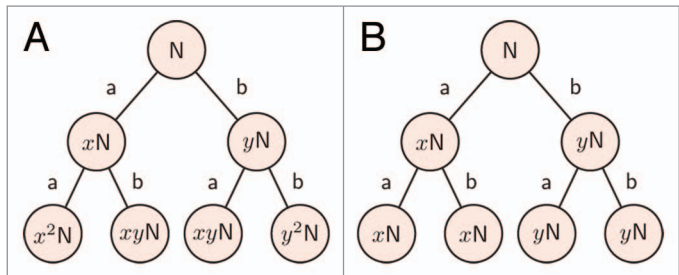

Figure 4. (**A**) Factor concentration patterns following repeated asymmetric cell divisions, given by g(a,b|kN), g(xkN|kN,a), g(ykN|kN,b). (**B**) For symmetric cell divisions, the content of the dividing cell is distributed equally to both daughters, resulting in identical factor concentrations, as described by g(a,b|kN), g(kN|kN).

In a cell lineage, division patterns like the ones described above will be repeated. Consider a cell containing a factor *N* at a given concentration. If *kN* is used to represent the factor concentration of the dividing cell, the concentration in each node following repeated cell divisions can be described by an iterated product (**Fig. 4A**)

$$g(a,b|kN),$$
$$g(xkN|kN,a),$$
$$g(ykN|kN,b).$$

With this notation a symmetric cell division (*m = n = 0.5*) is easily described through *x = y = 1*, giving both daughter cells identical factor concentrations (**Fig. 4B**)

$$g(a,b|kN),$$
$$g(kN|kN).$$

Asymmetric Tree Models for the E Lineage

Establishing model for wild-type behavior. Using the regulator functions from the previous section, we will now establish a general tree model of the asymmetric cell divisions in the E lineage of the nematode *C. elegans*. The model is general in the sense that we will not, at this stage, attempt to decipher the
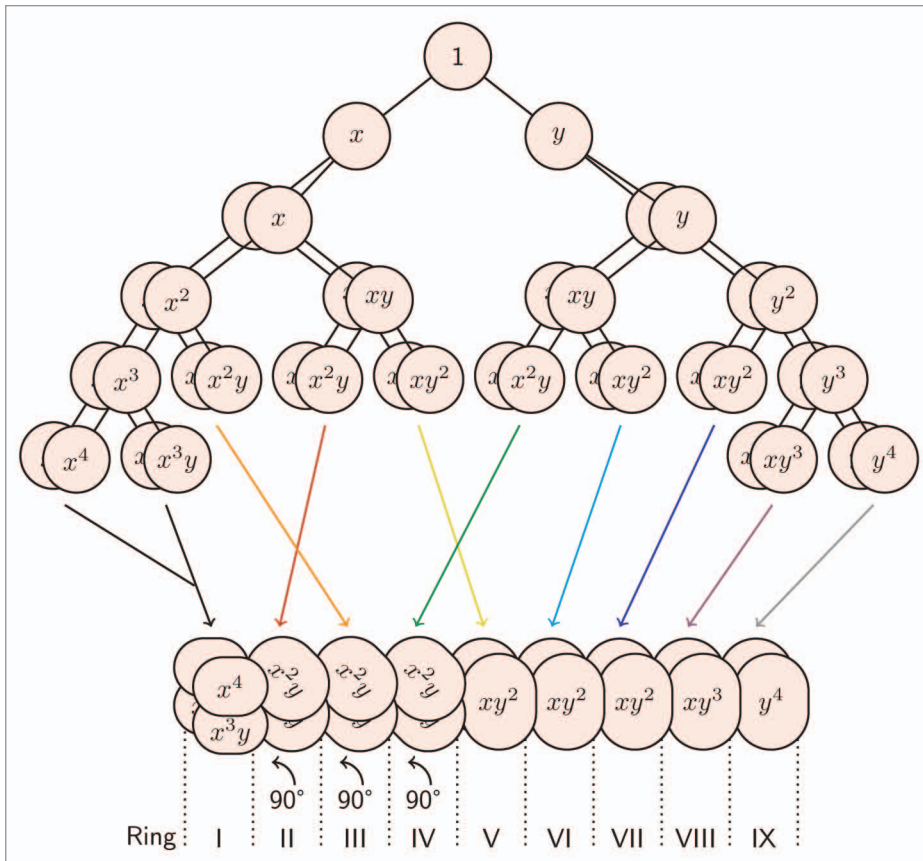
Figure 5. General tree model of the E lineage for wild-type embryos, describing the asymmetric distribution pattern of an arbitrary factor with an original concentration of one. There are six unique factor concentrations in the final cells. When transferred to the corresponding morphology of the intestine, we find that cells with identical factor concentrations are sorted next to each other (Rings II-IV and V-VII). Note that the second division in the lineage is symmetric. The regulators for this asymmetric distribution are g(x|a,–E2), g(y|b,–E2) and g(1|E2), where *E2* designates the symmetric division.

actual cell content or factors involved. Instead, we look at the general patterns that arise through iterated asymmetric divisions. In the following tree models, the cell division factors *a* and *b* are no longer explicitly portrayed. From this point on we also suppress the arbitrary factor *N* from the node expressions, highlighting the distribution patterns. Note that the second division in the lineage, occurring at the E2 stage along the left-right axis, is symmetric. Using the factor E2 to describe this division, the regulators governing asymmetric distribution are thus

$$g(x|a,-E2),$$
$$g(y|b,-E2),$$
$$g(1|E2).$$

With this notation, we introduce four assumptions:

(1) The asymmetry mechanism is equally effective in each cell division, regardless of tree location and/or factor concentration.

(2) The cell divisions in the E lineage are volume-symmetric.

(3) The factor concentrations of the two daughter cells are *x* times the initial concentration in the anterior cell and *y* times the initial concentration in the posterior cell, where $0 \leq x \leq 2$, $0 \leq y \leq 2$ and $x + y = 2$.

(4) For symmetric divisions, the factor concentrations of the two daughter cells are $x = y = 1$.

The first assumption above states that the mechanisms that generate the physical polarization of a given factor are not affected by the initial factor concentration or developmental stage. *C. elegans* embryos rely on several different ways to break symmetry during embryogenesis, differing between the germline and soma, so the asymmetry mechanisms are therefore not independent of tree location, i.e., lineage origin, in general.[23] However, once the E blastomere has been properly specified, the reiterated anterior-posterior asymmetry for the E lineage is upheld by the Wnt/β-catenin complex.[11,12,18,23] The second and third assumptions introduce the notation discussed in the previous section and sets the limits for *x* and *y*. We have found no reason to believe that cell divisions in the E lineage are volume-asymmetric. As mentioned previously, volume-asymmetric divisions can be modeled in a similar fashion, although the volumetric difference will affect the conditions for *x* and *y* set in (3)–(4). In the final assumption, the concentrations of a given factor are considered to be equal in the two daughter cells following a symmetric division. Importantly, this may lead to a completely altered cell fate compared with wild-type behavior. For instance, it is considered that cells adopt either an anterior or posterior cell fate following the inactivation of Wnt/β-catenin associated genes.[11,23]

To view the asymmetric distributions in their spatial context, the factor distributions from the tree model are transferred to the corresponding location in the intestine (**Fig. 5**). With one exception, the anterior half of the intestine, intestinal rings I-IV, is derived from the anterior Ea cell born at the E2 stage. The posterior-most Ea cells, Ealpp and Earpp, are however found in intestinal ring V, while the anterior-most Ep cells, Eplaa and Epraa, are located in ring IV. Looking at the factor concentrations for these cells, we find that the cells in rings IV and V are sorted with cells containing identical factor distributions. Notably, the switch in factor concentrations between ring IV and V coincides with the posterior limit for intestinal twist.

Establishing models for temperature sensitive *lit-1* mutants. It has been postulated that *lit-1* plays a role in defining the posterior limit of intestinal twist.[14] From this point on we will leave the general model and attempt to interpret the asymmetry patterns using published data concerning intestinal twist behavior in *lit-1* mutants. LIT-1 is an asymmetrically distributed protein that is
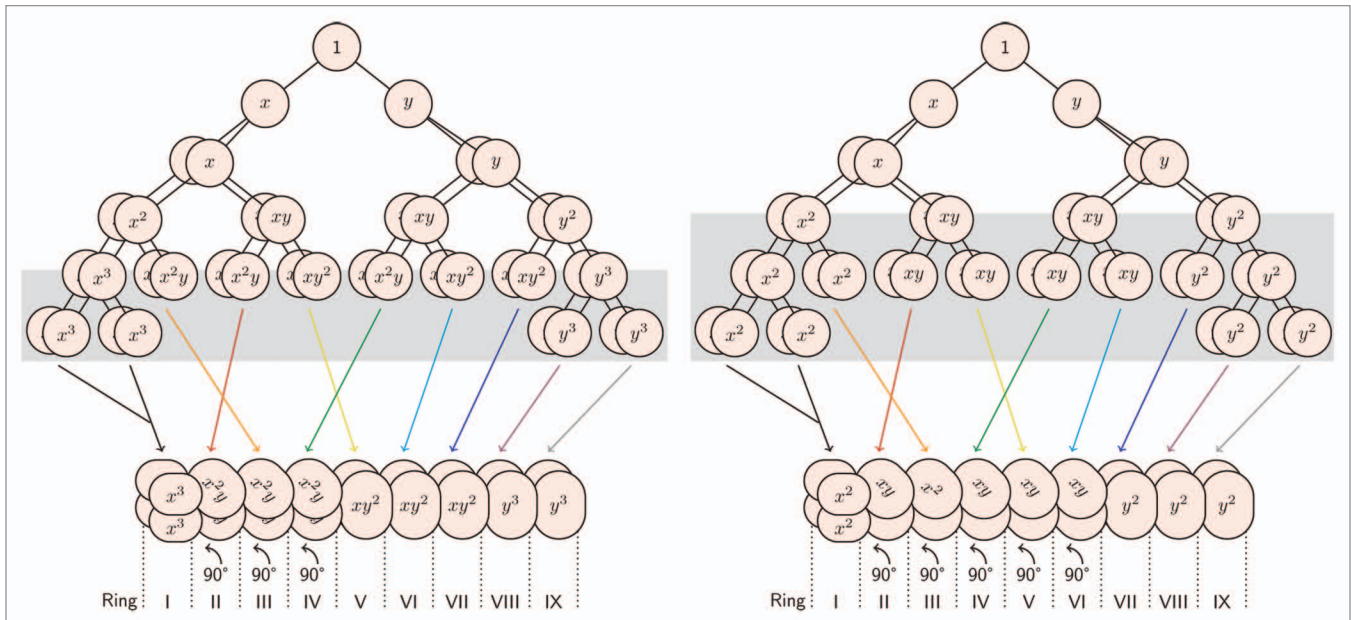
Figure 6. Tree models of the E lineage for temperature sensitive mutants moved to a non-permissive temperature at the (**A**) E16 and (**B**) E8 stage of intestinal development. All cell divisions following the activation of the temperature sensitive mutations are considered symmetric (gray zone). The resulting factor distributions are transferred to the corresponding intestinal morphology of *lit-1* mutants, displaying twist patterns as reported by Hermann et al.[14] Note that the second division in the lineage is always symmetric.

part of a general polarity complex, including WRM-1, SYS-1 and POP-1, that establishes asymmetry in embryonic cell divisions by influencing the location and transcriptional activity of POP-1, a TCF-related transcription factor.[17,18,23] Its role in intestinal twist has been elucidated by examining twist behavior in temperature-sensitive *lit-1* mutants moved to a non-permissive temperature at the E8 and the E16 stages of development.[14] By assuming that all cell divisions following the activation of the mutation are symmetric, we first establish general asymmetry models for these two mutants (**Fig. 6**).

The model for the E16 mutant (**Fig. 6A**) largely displays the same factor distributions as the wild-type model (**Fig. 5**), with the exception of the peripheral rings. This is expected since the last round of division only occurs in the cells that make up these rings (Ints I, VIII and IX). For the E8 mutant, the distribution pattern differs notably from the wild-type model, with intestinal rings II, IV, V and VI sharing the same factor concentrations (**Fig. 6B**). As previously stated, the switch in factor distribution between intestinal rings IV and V in wild-type embryos coincides with the posterior limit of intestinal twist. For the embryos where the mutation was activated at the E8 stage (E8 *lit-1* mutants), Hermann et al. reported that not only Int II-IV, but rings up to and including Int VI, rotated.[14] The corresponding model for this mutant illustrates a switch in factor concentrations between ring VI and VII, again coinciding with the posterior boundary for the observed twist (**Fig. 6B**). The E16 *lit-1* mutants follow a wild-type behavior up until the last cell division. For these embryos, intestinal twist was reported to extend beyond intestinal ring V in 5% of the studied cases. This observation could be explained if some of the embryos were switched to the non-permissive temperature

before entering the E16 stage, i.e., while still in the late E8 stages.

It is important to note that LIT-1 may not necessarily be the crucial factor in itself. The effects of the asymmetric factor distributions may well be coupled to an associated protein, such as the transcription factor POP-1 or the downstream result of various ratios in this Wnt/β-catenin regulator complex.[11,12,14]

A factor concentration switch coincides with posterior limit of intestinal twist—Implications for a threshold mechanism. The correlation between the asymmetric distribution patterns in our model and the observed twist behavior allows for speculation on whether twist occurs in cells where the factor distributions (of LIT-1 or an associated factor) cross some threshold. If that is the case, the existing data should reveal clues as to what the potentially critical concentration would be. We therefore plot the factor distributions over x, using $y = 2 - x$, to compare these results with the observed twist behavior (**Fig. 7**). Since wild-type embryos and E16 *lit-1* mutants (**Fig. 7A**) share factor distributions in the rotating rings they will be discussed together. In wild-type and *lit-1* E16 mutant embryos, cells with factor concentration x^2y rotate, whereas cells with xy^2 do not (**Fig. 7B**). By assuming that twist occurs in intestinal rings where cellular factor distributions are above a certain threshold T, we state that $xy^2 \leq T \leq x^2y$, where it follows that $y \leq x$. Similarly, for the E8 *lit-1* mutants (**Fig. 7C and D**), cells with factor concentrations of xy or x^2 rotate while cells with y^2 do not. Thus, we add $T \leq xy$.

For wild-type embryos, the upper and lower boundaries for twist are set by xy^2 and x^2y. If we assume that the system is most stable if the critical concentration lies in the middle of the region between these two boundaries, the threshold should be given by the mean of these curves, which corresponds to xy. According
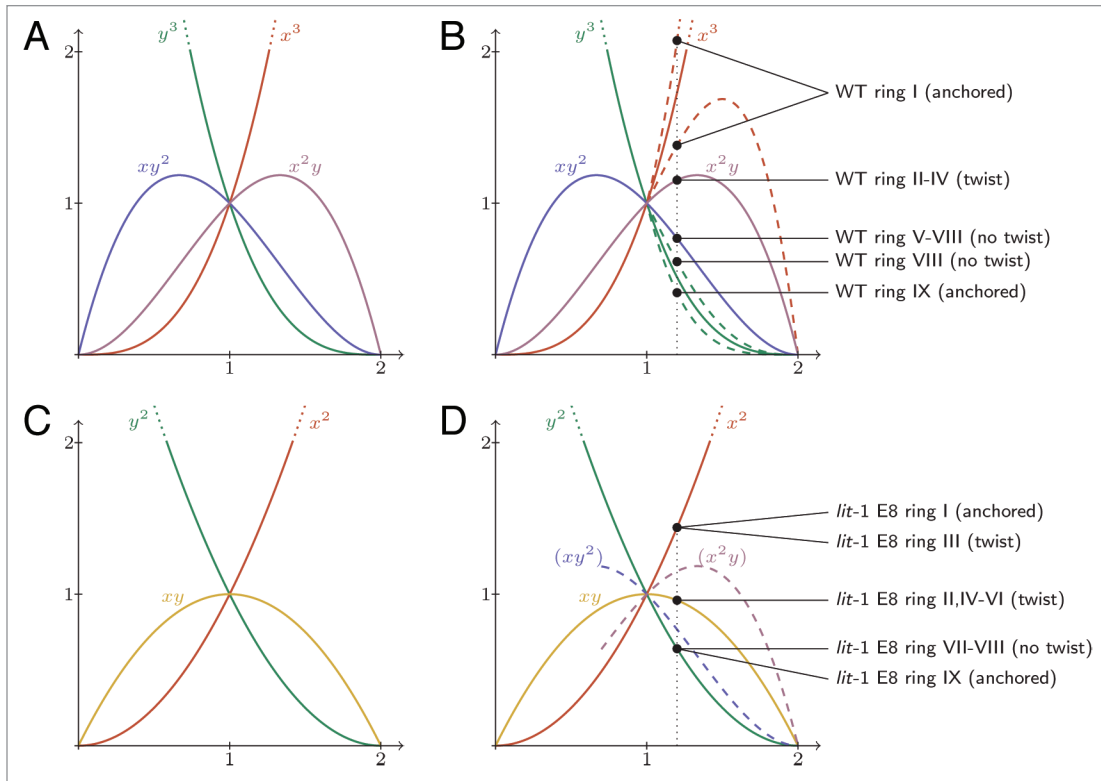
Figure 7. Plot of the factor distributions over x, using $y = 2 - x$, for the E16 *lit-1* (**A and B**) and E8 *lit-1* (**C and D**) mutants. The E16 mutant closely follows wild-type behavior (**B**), where cells with factor concentrations x^2y rotate, while those with xy^2 and xy^3 do not. In E8 *lit-1* mutants (**D**), cells with factor concentrations x^2 and xy rotate, whereas those with y^2 do not.
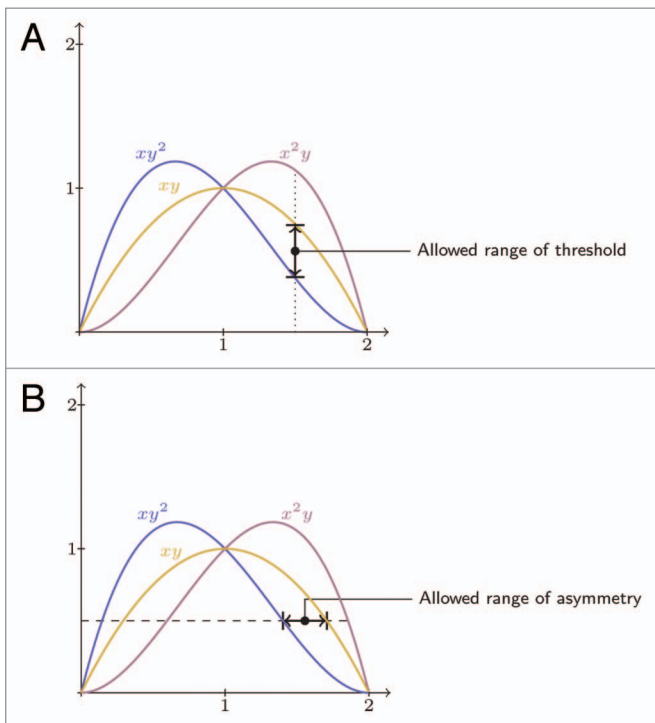

Figure 8. Plot of the factor distributions over x, using $y = 2 - x$. (**A**) Based on observed behavior, the potential critical concentration for intestinal twist lies between xy and xy^2.[2] Thus, the allowed range of the threshold is given by these curves. (**B**) Analogously, a given concentration (threshold) gives us the allowed range of asymmetry.

to observations from the E8 *lit-1* embryo, cells with this factor concentration will rotate. Therefore, the allowed range of the threshold lies between xy^2 and xy (**Fig. 8A**). A similar approach can be used to define the allowed range of asymmetry (**Fig. 8B**). For a given threshold, the factor concentration in the anterior daughter (i.e., x) must lie within this range in order to uphold the observed twist pattern.

Establishing models for all possible mutation patterns in the E lineage. Given that intestinal twist is indeed governed by a threshold mechanism, the meta-Boolean model should be able to predict the twist outcome of theoretical mutants. To explore this, we first establish a list of all possible combinations for symmetric and asymmetric divisions in the E lineage. In total, there are five divisions in the E lineage. Since the second division occurs along the left-right axis and is always symmetric, there are a total of 2^4 possible combinations of division patterns in the lineage, all of which are illustrated in **Table 1**. Here, mutant A corresponds to the wild-type embryo, mutant B to a mutant shifted to a nonpermissive temperature, or corresponding mutant activation, at the E16 stage and mutant D corresponds to a mutant shifted at the E8 stage. As mentioned previously, the factor distributions for wild-type (mutant A) and E16 mutants (mutant B) are identical

with the exception of three intestinal rings (I, VIII and IX). By looking at **Table 1** it is clear that the only difference between them is the final round of division at the E16 stage. Analogously, all subsequent pairs (C + D, E + F, etc.) follow the same pattern and will thus have identical factor distributions in six of the intermediate rings.

We then establish lineage tree models for each of these combinations. Interestingly, we find that each one gives rise to a unique distribution pattern (**Fig. 10**). There are 10 unique factor concentrations in the intermediate rings for the various mutants. Seven of these have already been addressed (**Fig. 7**). For the remaining three concentrations, x, y and 1, both x and 1 are well above the upper boundary set by xy for $1 \leq x \leq 2$, and are therefore not discussed further, however, y cuts right through the range of interest for the critical concentration (**Fig. 9**). In this case, the ratio between x and y, i.e., the efficiency of the asymmetry mechanism, becomes important. If x is only slightly larger than 1, the curve for y follows that of xy^2 closely. However, for larger values of x, this is no longer the case. The predicted outcome for cells with this factor concentration thus becomes a question of how stable the system is in terms of the threshold and how efficient the asymmetry mechanism is, according to our previous discussion (**Fig. 8**).

Model Based Predictions and Experimental Designs

With the exception discussed above, the factor concentrations in **Figure 10** can now be related to the existing boundaries, set by xy and $xy.^2$ Since the peripheral rings (Int I and IX) are anchored to the intestinal valves, we will limit our observations to the intermediate rings (Int II-VIII) when we compare the asymmetric distribution patterns with intestinal twist behavior. The factor distributions for each of the theoretical mutants are presented in **Figure 10**. All cells containing concentrations above the upper limit set by xy are shaded red, while those with concentrations below the lower limit set by xy^2 are shaded blue. Cells with the final, unknown concentration y are shaded purple. In **Figure 10**, we have, to begin with, assumed that (1) y falls below the threshold and that these cells will not rotate and (2) that all cells with concentrations equal to or above xy will rotate, regardless of neighboring cells. These assumptions will be addressed in more detail below, where we will discuss what various experimental outcomes would imply regarding the mechanisms of intestinal twist.

Determining the threshold. The unique patterns of the mutants in **Figure 10** enable us to speculate on the various twist patterns for these mutants and address some of the mechanisms that regulate the limit of this morphological event. Let us first address the remaining, unknown factor concentration y. This can be further investigated by studying the twist behavior of, for example, mutant G. In **Figure 10**, the twist behavior for this mutant is based on the assumption that y falls below the threshold and that these cells will not twist (**Fig. 11, G**). If instead y is above the threshold, the factor distributions will rise above the threshold for all rings in the intestine and mutant G will thus follow the patterns of mutants O or P for the intermediate rings (**Fig. 11, G'**).

Table 1. Listing of all possible combinations for asymmetric (ON) and symmetric (OFF) divisions in the E lineage

Mutant	E	E2	E4	E8	E16
A	ON	OFF	ON	ON	ON
B	ON	OFF	ON	ON	OFF
C	ON	OFF	ON	OFF	ON
D	ON	OFF	ON	OFF	OFF
E	ON	OFF	OFF	ON	ON
F	ON	OFF	OFF	ON	OFF
G	ON	OFF	OFF	OFF	ON
H	ON	OFF	OFF	OFF	OFF
I	OFF	OFF	ON	ON	ON
J	OFF	OFF	ON	ON	OFF
K	OFF	OFF	ON	OFF	ON
L	OFF	OFF	ON	OFF	OFF
M	OFF	OFF	OFF	ON	ON
N	OFF	OFF	OFF	ON	OFF
O	OFF	OFF	OFF	OFF	ON
P	OFF	OFF	OFF	OFF	OFF

E, E2, E4, E8 and E16 describe the various stages in the E lineage development. Note that the second cell division in the lineage is always symmetric. The resulting theoretical mutants are designated A–P for the remainder of this paper.
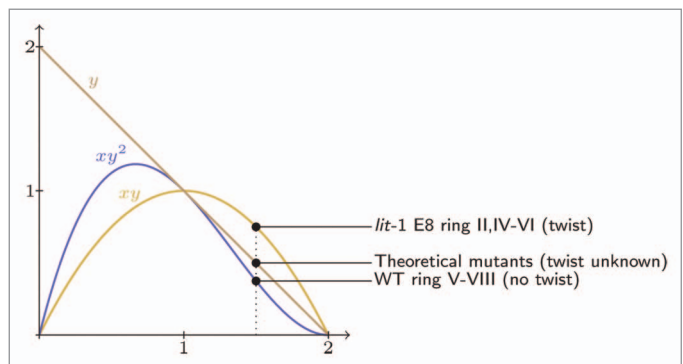

Figure 9. Plot of the factor distributions over x, using $y = 2 - x$. The highest concentration for non-twisting cells is xy^2, whereas the lowest concentration for twisting cells is xy. With one exception, y, the remaining factor concentrations for the theoretical mutants are either below or above these boundaries.

Determining whether factor concentration is sufficient for intestinal twist. According to our initial assumption, the twist patterns in **Figure 10** are obtained if cellular concentration alone is enough for intestinal twist to occur. Several mutants display a pattern where cells with factor concentrations above and below the threshold are intermingled. For mutant I, the factor concentrations in intestinal ring V fall below the threshold, while cells in neighboring rings all have factor concentrations above or equal to xy. The twist behavior of this mutant can follow several patterns and the outcome will answer whether factor concentration alone is sufficient for intestinal twist. First, as **Figure 10** implies, twist
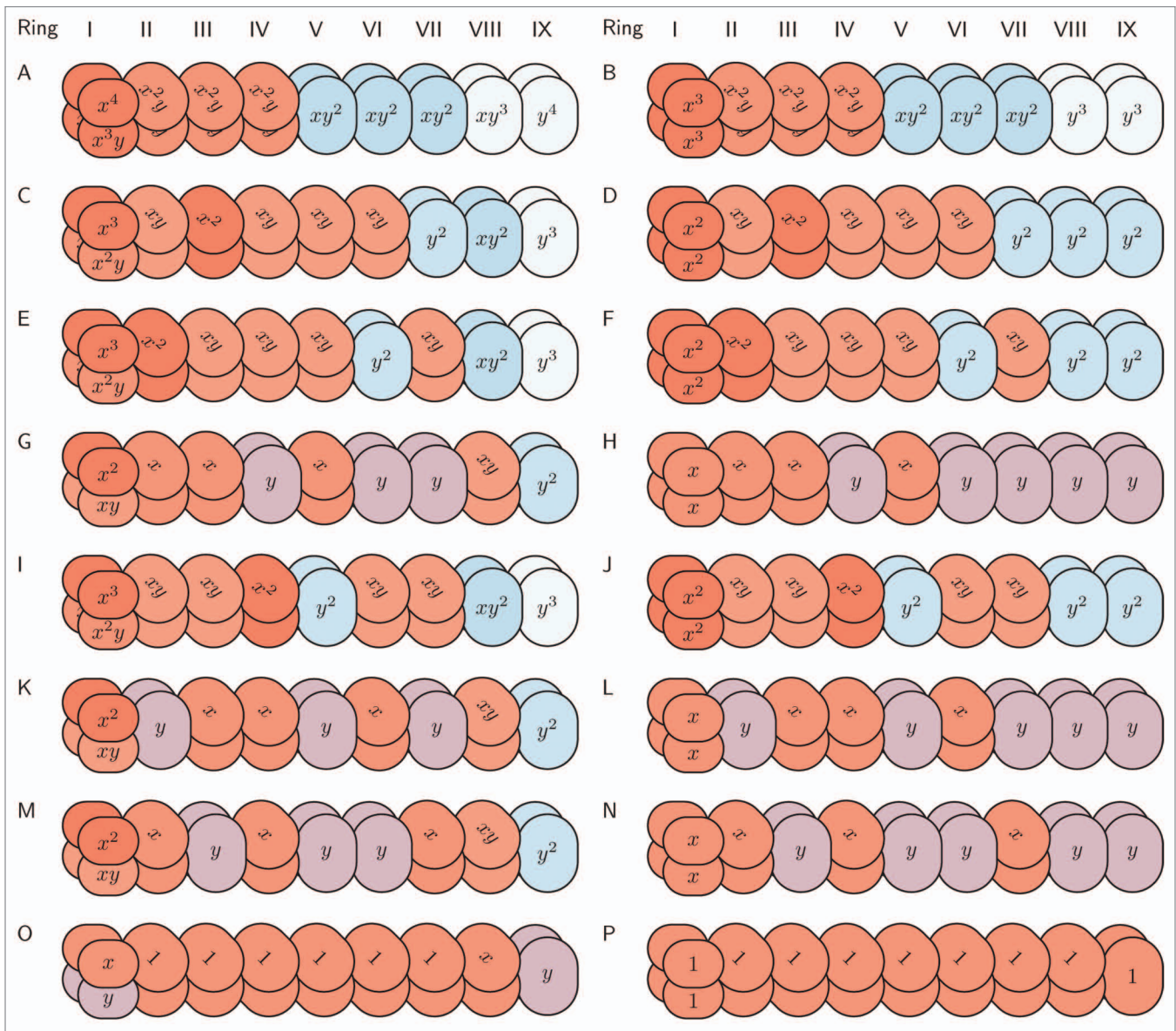
Figure 10. Factor concentrations for all possible combinations of symmetric and asymmetric divisions in the E lineage, according to the division patterns set in **Table 1**. Cells with factor concentrations above or equal to the upper limit set by xy are shaded red, while cells with factor concentrations below or equal to the lower limit set by xy^2 are shaded blue. Cells with the factor concentration y, are shaded purple. In this figure, intestinal twist patterns are shown with the assumptions that $y < T$ and that cellular concentration alone is enough for twist to occur. I–IX describe the intestinal rings with anterior to the left and posterior to the right. A–P denotes the mutant asymmetry patterns established in **Table 1**.

may occur in all cells with factor concentrations above the threshold (**Fig. 12, I**). It is also possible that twist could occur in all cells up until the first cell (from the anterior end) that falls below the threshold, i.e., ring V (**Fig. 12, I'**). Alternatively, considering a case where cells on both sides of intestinal ring V rotate, it is possible that the cells in Int V may twist due to neighbor influence, such as for example cell mechanical forces (**Fig. 12, I"**).

Determining the mechanisms of anterior-posterior progression of twist. The twist behavior in **Figure 12, I'** is obtained if an unbroken chain of cells with concentrations above the threshold is required for twist to occur. Such mechanisms can be studied by comparing the twist patterns of mutants K, M and G (**Fig. 13**).

The first three rows of **Figure 13** describe these mutants according to the previous assumptions (K, M and G), whereas the final three rows show a pattern where twist occurs for all rings up to the first encounter with a ring where the factor concentrations fall below the threshold (K', M' and G'). Here we have assumed that y is below the threshold and that twist does not occur cell-autonomously. For example, if there is no intestinal twist in mutant K, while intestinal ring II rotates in mutant M, and rings II-III rotate in mutant G, contact with ring I is most likely crucial. This would also imply that a combination of asymmetric concentrations and cell-to-cell contacts work together to set the limit for intestinal twist.

To summarize, the division patterns listed in **Table 1** and the corresponding factor concentrations in **Figure 10** can be used as a basis for experiments that may help answer some of the unanswered questions regarding intestinal twist, given that the experimental challenges (see sections below) can be solved. In the current manuscript we have given some examples of possible experiments. For example, by studying the twist behavior for any mutant containing rings with the unknown factor concentration y (i.e., mutants G–H and/or K–N) the allowed threshold range can be further narrowed (see **Fig. 11**). In addition, any mutant where cells containing factor concentrations above and below the theoretical threshold are intermixed, such as mutants E–N, can be used to study whether intracellular factor concentration alone is sufficient for twist to occur (see **Fig. 12**). Finally, by comparing mutants K, G and M, the mechanisms behind the anterior-posterior progression of twist can be investigated (see **Fig. 13**).

Possible effects outside the E lineage. As mentioned previously, mutants B and D correspond to the E16 and E8 *lit-1* mutants. In these cases, switching the embryos to a non-permissive temperature activates the mutation. In our model, this corresponds to a division pattern that switches from ON (where asymmetric cell divisions are active) to OFF (where all subsequent divisions are considered symmetric). For this type of straightforward ON-to-OFF mutants, only two examples remain—mutant H, which corresponds to a mutation activated at the E4 stage, and mutant P, activated at the E blastomere stage (**Table 1**). However, since LIT-1 is part of a general polarity complex that is active during embryogenesis, activating the mutation at such early stages of development could compromise the outcome of intestinal twist in other ways.[11,24] For example, anterior-posterior asymmetry is needed in the MS lineage to allow for the Notch signal that distinguishes the left- and right-hand side of the intestine at the E4 stage. Should this be altered, the bilateral asymmetry in the intestine is compromised, which in turn would lead to intestinal twist failure.[14] Mutant P, where the entire E lineage is developed through symmetric cell divisions, is an example of this. According to the initial assumption (**Fig. 10**), twist will occur along the entire intestine (**Fig. 14, P**), yet the more likely outcome will be a non-twisting intestine (**Fig. 14, P′**).

Possible experimental difficulties. In combination with the model results, the theoretical mutants in **Table 1** directly translate into a series of proposed experiments. These are beyond the scope of this article, but we hope to be able to test these predictions in association with an experimental collaborator in future work. Experiments that involve a switch from OFF (where the asymmetry has been prevented) to ON (where asymmetry is restored) need mutant rescue mechanisms to be testable. This includes reversible LIT-1 mutants, where both activation and deactivation of the mutation must occur within the time frame of a cell division cycle. In addition, there are timing issues to be considered in regards to these experiments, in order to ensure that the mutation is activated and/or rescued at the correct developmental stages without disturbing, or at least minimizing the effect on, normal embryogenesis during monitoring. Finally, the ideal organism would restrict the mutation to the E lineage in order to avoid affecting anterior-posterior patterns in the rest of
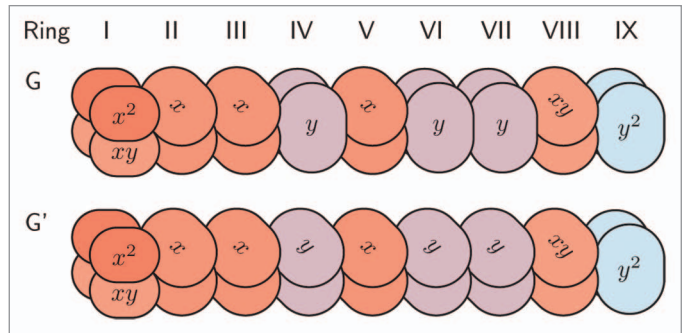

Figure 11. The remaining unknown factor concentration y can be further investigated by studying the twist patterns for mutants with this concentration, such as for example mutant G. The above figure illustrates two scenarios where y is either $< T$ (G) or $> T$ (G′) respectively, again with the general assumption that cell concentration alone is enough for twist to occur. These results would help further narrow the allowed range for T (**Fig. 8**).
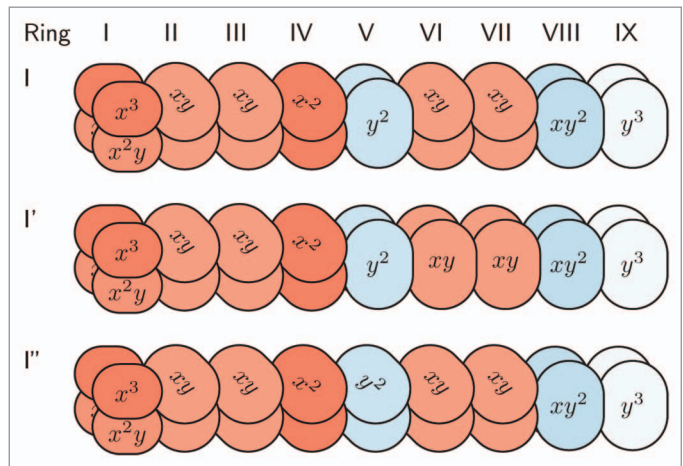

Figure 12. Mutants where cells with factor concentrations above and below T are intermingled can be used to investigate whether or not intracellular concentration is in fact enough to induce intestinal twist. The above example shows various twist patterns for mutant I, where twist occurs for all cells with factor concentrations $> T$ (I), for all cells up to the first ring where the factor concentration $< T$ (I′) or for all cells up until the last ring with factor concentration $> T$ (I″). In the latter case, there is also a possibility that mechanical forces from neighboring cells may influence the twist patterns (I″).

the embryo. If these limitations can be overcome, the observed twist behavior of these mutants, in combination with the unique patterns that arise from each respective tree model, will provide answers to some of the remaining questions regarding intestinal twist mechanisms, according to our previous discussion.

Discussion

The model that we present here is general in the sense that the factor concentrations for the various mutants (**Fig. 10**) are valid for all factors that comply with the assumptions set previously (I–IV). In its current form, the model describes a sequential
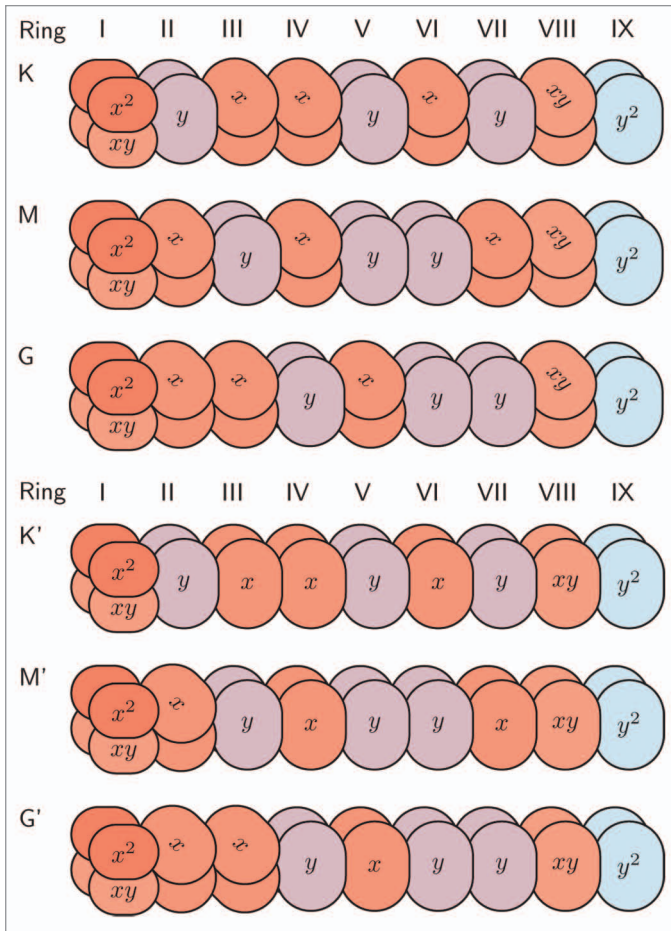
Figure 13. Mutants K, M and G can be used to study whether cell-to-cell contacts are needed for the progression of intestinal twist. The first three rows show twist patterns according to the assumptions in **Figure 10 (K, M and G)**, i.e., that $y < T$ and that intracellular factor concentration alone is enough to induce twist. The final three rows show the twist pattern as they would appear if an unbroken chain of cells with concentrations $> T$ in contact with Int I is required for twist to occur (K', M' and G'). In this latter case, intracellular concentration is thus not enough to induce twist.
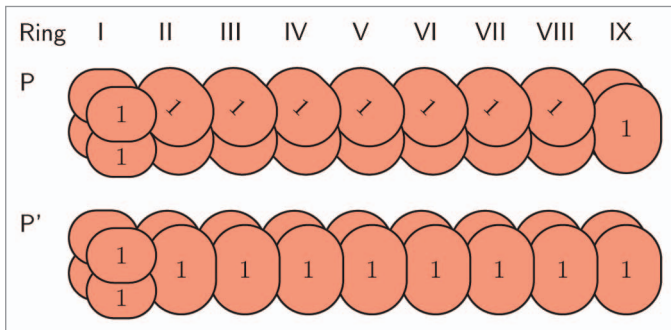

Figure 14. Twist patterns of mutant P according to the assumption that all cells with factor concentrations $> T$ will twist (P) or the more likely event of twist failure due to early *lit-1* inactivation (P').

production of factors that is lineage-autonomous, i.e., determined by the cell's location in the lineage tree, provided that the E blastomere has been properly specified in the early embryo. In support of this approach, others have shown that the anterior-posterior patterning of the anterior endoderm is unaffected by non-endodermal cells during these conditions, and it has been speculated that anterior-posterior patterns within other cell lineages are the result of polarity relay mechanisms.[12,25] Disturbing the anterior-posterior patterning of early blastomeres, by blocking or otherwise manipulating the transcriptional activity of the POP-1 transcription factor, can lead to significant cell fate changes and could well affect a given cell's ability to induce and/or respond to extracellular cues, such as membrane-bound proteins, paracrine signaling or chemotactic gradients.[17,19] Thus, cell fate decisions depending on such events could in part be influenced by an initial anterior-posterior asymmetry.

The meta-Boolean approach used in this study is a rule-based, low-complexity, deterministic model. These types of models can be built around qualitative knowledge of a biological system and do not necessarily require quantitative information, such as molecular concentrations or kinetic parameters.[26] As a result, the granularity of these models is coarse to at best average. For smaller well-characterized systems, where there is ample quantitative data, more fine-grained models such as nonlinear ordinary differential equations may be more useful, but these will, by their nature, become more computationally complex.[27] For larger systems, a comprehensive model that describes the entire system may become not only computationally challenging, but also difficult to interpret in terms of the generated data.[27] In these cases, there are options. A large system can for instance be divided into smaller, functional modules that are initially modeled on their own and subsequently added to a larger, system-wide model. Alternatively, a hierarchy of models can be used to describe the different characteristics of a large system on different abstraction levels.[27]

One of the strengths with the meta-Boolean approach is its ability to discover general and large-scale patterns in cell lineages using a minimal amount of model factors.[20] Even in its current form, the model has yielded several predictions and experimental suggestions, including some that do not involve exclusively lineage-autonomous events. Consider for example **Figure 13**. Here, one interpretation of the model (K', G' and M') implies that actual cell-to-cell contact between cells containing factor concentrations above the threshold is required to progress twist along the intestine. In line with the previously mentioned hierarchy strategy, it is also possible to extend the present model gradually to describe the cellular events of intestinal twist on various abstraction levels. The meta-Boolean model approach can for instance incorporate external influences through its use of general model factors.

Conclusions

In the current study we have established a general model describing anterior-posterior asymmetry patterns in the E lineage of *C. elegans*, including asymmetric distribution models for all possible combinations of symmetric and asymmetric divisions

in this lineage. In addition, a potential threshold mechanism has been discussed by comparing the factor distributions from our model with observed twist behavior in *lit-1* mutants. The emerging distribution patterns may help explain the previously identified dependence between *lit-1* activity and the posterior boundary of intestinal twist. If the experimental challenges that are associated with *lit-1* rescue mutants can be overcome, the presented models could be used to identify some of the underlying mechanisms of intestinal twist.

References

1. Leung B, Hermann GJ, Priess JR. Organogenesis of the Caenorhabditis elegans intestine. Dev Biol 1999; 216:114-34; PMID:10588867; http://dx.doi.org/10.1006/dbio.1999.9471.

2. Sulston JE, Schierenberg E, White JG, Thomson JN. The embryonic cell lineage of the nematode Caenorhabditis elegans. Dev Biol 1983; 100:64-119; PMID:6684600; http://dx.doi.org/10.1016/0012-1606(83)90201-4.

3. Deppe U, Schierenberg E, Cole T, Krieg C, Schmitt D, Yoder B, et al. Cell lineages of the embryo of the nematode Caenorhabditis elegans. Proc Natl Acad Sci U S A 1978; 75:376-80; PMID:272653; http://dx.doi.org/10.1073/pnas.75.1.376.

4. Junkersdorf B, Schierenberg E. Embryogenesis in *C. elegans* after elimination of individual blastomeres or induced alteration of the cell division order. Rouxs Arch Dev Biol 1992; 202:17-22; http://dx.doi.org/10.1007/BF00364593.

5. Maduro MF. Structure and evolution of the C. elegans embryonic endomesoderm network. Biochim Biophys Acta 2009; 1789:250-60; PMID:18778800; http://dx.doi.org/10.1016/j.bbagrm.2008.07.013.

6. Rocheleau CE, Downs WD, Lin R, Wittmann C, Bei Y, Cha YH, et al. Wnt signaling and an APC-related gene specify endoderm in early C. elegans embryos. Cell 1997; 90:707-16; PMID:9288750; http://dx.doi.org/10.1016/S0092-8674(00)80531-0.

7. Goldstein B. Induction of gut in Caenorhabditis elegans embryos. Nature 1992; 357:255-7; PMID:1589023; http://dx.doi.org/10.1038/357255a0.

8. Goldstein B. Establishment of gut fate in the E lineage of C. elegans: the roles of lineage-dependent mechanisms and cell interactions. Development 1993; 118:1267-77; PMID:8269853.

9. Fukushige T, Hawkins MG, McGhee JD. The GATA-factor elt-2 is essential for formation of the Caenorhabditis elegans intestine. Dev Biol 1998; 198:286-302; PMID:9659934.

10. McGhee JD, Sleumer MC, Bilenky M, Wong K, McKay SJ, Goszczynski B, et al. The ELT-2 GATA-factor and the global regulation of transcription in the C. elegans intestine. Dev Biol 2007; 302:627-45; PMID:17113066; http://dx.doi.org/10.1016/j.ydbio.2006.10.024.

11. Kaletta T, Schnabel H, Schnabel R. Binary specification of the embryonic lineage in Caenorhabditis elegans. Nature 1997; 390:294-8; PMID:9384382; http://dx.doi.org/10.1038/36869.

12. Schroeder DF, McGhee JD. Anterior-posterior patterning within the Caenorhabditis elegans endoderm. Development 1998; 125:4877-87; PMID:9811572.

13. Fukushige T, Goszczynski B, Yan J, McGhee JD. Transcriptional control and patterning of the pho-1 gene, an essential acid phosphatase expressed in the C. elegans intestine. Dev Biol 2005; 279:446-61; PMID:15733671; http://dx.doi.org/10.1016/j.ydbio.2004.12.012.

14. Hermann GJ, Leung B, Priess JR. Left-right asymmetry in C. elegans intestine organogenesis involves a LIN-12/Notch signaling pathway. Development 2000; 127:3429-40; PMID:10903169.

15. Neves A, English K, Priess JR. Notch-GATA synergy promotes endoderm-specific expression of ref-1 in C. elegans. Development 2007; 134:4459-68; PMID:18003741; http://dx.doi.org/10.1242/dev.008680.

16. Neves A, Priess JR. The REF-1 family of bHLH transcription factors pattern C. elegans embryos through Notch-dependent and Notch-independent pathways. Dev Cell 2005; 8:867-79; PMID:15935776; http://dx.doi.org/10.1016/j.devcel.2005.03.012.

17. Lin R, Hill RJ, Priess JR. POP-1 and anterior-posterior fate decisions in C. elegans embryos. Cell 1998; 92:229-39; PMID:9458047; http://dx.doi.org/10.1016/S0092-8674(00)80917-4.

18. Mizumoto K, Sawa H. Two betas or not two betas: regulation of asymmetric division by beta-catenin. Trends Cell Biol 2007; 17:465-73; PMID:17919911; http://dx.doi.org/10.1016/j.tcb.2007.08.004.

19. Huang S, Shetty P, Robertson SM, Lin R. Binary cell fate specification during C. elegans embryogenesis driven by reiterated reciprocal asymmetry of TCF POP-1 and its coactivator beta-catenin SYS-1. Development 2007; 134:2685-95; PMID:17567664; http://dx.doi.org/10.1242/dev.008268.

20. Larsson JK, Wadströmer N, Hermanson O, Lendahl U, Forchheimer R. Modelling cell lineage using a meta-Boolean tree model with a relation to gene regulatory networks. J Theor Biol 2011; 268:62-76; PMID:20946901; http://dx.doi.org/10.1016/j.jtbi.2010.10.003.

21. McGhee JD. The C. elegans intestine. WormBook 2007; •••:1-36; PMID:18050495.

22. Maduro MF, Rothman JH. Making worm guts: the gene regulatory network of the Caenorhabditis elegans endoderm. Dev Biol 2002; 246:68-85; PMID:12027435; http://dx.doi.org/10.1006/dbio.2002.0655.

23. Munro E, Bowerman B. Cellular symmetry breaking during Caenorhabditis elegans development. Cold Spring Harb Perspect Biol 2009; 1:a003400; PMID:20066102; http://dx.doi.org/10.1101/cshperspect.a003400.

24. Rocheleau CE, Yasuda J, Shin TH, Lin R, Sawa H, Okano H, et al. WRM-1 activates the LIT-1 protein kinase to transduce anterior/posterior polarity signals in C. elegans. Cell 1999; 97:717-26; PMID:10380924; http://dx.doi.org/10.1016/S0092-8674(00)80784-9.

25. Bischoff M, Schnabel R. A posterior centre establishes and maintains polarity of the Caenorhabditis elegans embryo by a Wnt-dependent relay mechanism. PLoS Biol 2006; 4:e396; PMID:17121454; http://dx.doi.org/10.1371/journal.pbio.0040396.

26. Wang RS, Saadatpour A, Albert R. Boolean modeling in systems biology: an overview of methodology and applications. Phys Biol 2012; 9:055001; PMID:23011283; http://dx.doi.org/10.1088/1478-3975/9/5/055001.

27. de Jong H. Modeling and simulation of genetic regulatory systems: a literature review. J Comput Biol 2002; 9:67-103; PMID:11911796; http://dx.doi.org/10.1089/10665270252833208.